Preparation and Properties of Surface-Conductive Polyimide Films via In Situ Codeposition of Metal Salts

J. D. Rancourt and L. T. Taylor*

Department of Chemistry, Virginia Polytechnic Institute and State University, Blacksburg, Virginia 24061. *Received May 9, 1986*

ABSTRACT: Polyimides, due to their high thermal stability, excellent chemical stability, and useful mechanical properties, are utilized in aerospace, electronic, and specialty consumer markets. Though normally the polyimides are used because of their high electrical resistivity in some applications (conductive adhesives and inks, EMI and RFI shielding) low electrical resistivity is desirable. Toward this goal polyimides have been modified with metal salts and metal complexes. Ionic species uniformly distributed throughout the bulk of the film or highly anisotropic structures containing near-surface metal or metal oxide are obtained, depending upon the processing conditions. In this study the surface conductivity of a polyimide containing surface cobalt has been increased by utilizing codoping techniques. Data pertaining to cobalt-doped and cobalt/lithium-codoped condensation polyimides are presented.

Introduction

An interdisciplinary research program to develop materials having the high thermal stability and useful engineering properties characteristic of polyimides but having substantially altered electrical properties is in progress. By modifying polyimides with various metal salts and metal complexes our research group has obtained materials having metallic,[1] semiconductive,[2] and photoconductive[2] surfaces. For example, homogeneous incorporation of an appropriate soluble cobalt salt or lithium salt into poly(amic acid) solutions (polyimide precursor) with subsequent thermal curing yields condensation polyimide films having a semiconductive cobalt oxide surface[3,4] or a lithium oxide surface.[5] In each case the air-side electrical resistivity is more dramatically reduced than the volume resistivity relative to the nondoped polymer. Information from surface-sensitive spectroscopic techniques and a variety of electrical measurements has been used to propose a structural model that represents the metal ion modified polyimide films in terms of both their spectroscopic properties and dc electrical resistivity.[6] In addition, a deeper understanding of the surface characteristics of these novel materials has guided additional research. In this regard, reportedly a small amount of lithium oxide stoichiometrically substituted for cobalt(II) in cobalt oxide (Co_3O_4) greatly enhances the electrical conductivity of the resulting mixed oxide relative to the pure cobalt oxide.[7,8] In an attempt to obtain a lower resistivity lithium-substituted cobalt oxide semiconductive surface on condensation polyimide films we prepared and evaluated polyimide films that have been codoped with lithium chloride and cobalt chloride.[9] Electrical, thermal, and spectroscopic data obtained on the codoped systems will be compared and contrasted to a polyimide individually doped with either cobalt chloride or lithium chloride.

Experimental Section

Chemicals. 3,3′,4,4′-Benzophenonetetracarboxylic dianhydride (BTDA, Aldrich Chemical Co.) was vacuum dried at 100 °C for 2 h. 4,4′-Oxydianiline (ODA, Aldrich Chemical Co.) was sublimed at 185 °C and less than 1 Torr. HPLC grade *N,N*-dimethylacetamide (DMAc, Aldrich Chemical Co.) was stored over molecular sieves under a nitrogen atmosphere and sparged with dry nitrogen prior to use. Anhydrous cobalt(II) chloride was prepared by heating cobalt(II) chloride hexahydrate for 3 h at 120 °C under vacuum. Anhydrous lithium chloride was obtained from commercial sources and used after drying in a vacuum oven for ~24 h at 110 °C.

Polymer Synthesis and Modification. The condensation reaction between the dianhydride and the diamine was performed in *N,N*-dimethylacetamide at room temperature. For example ODA (0.004 mol) was added to a nitrogen-purged glass septum bottle with 7 mL of DMAc. The dianhydride (0.004 mol) was then added to the diamine solution with an additional milliliter of DMAc, resulting in 22 wt % polymer concentration. The resulting solution was stirred for 20–24 h to form the poly(amic acid) (polyimide precursor). For the cobalt-modified or lithium-modified polyimides anhydrous cobalt(II) chloride or lithium chloride (0.001 mol) was added as a solid within 0.5 h after the dianhydride. For lithium-codoped films anhydrous lithium chloride (0.5, 0.05, or 0.005 mmol) was added to a poly(amic acid) solution containing 0.001 mole of anhydrous cobalt chloride.

Film Preparation. Poly(amic acid) solutions were centrifuged at ca. 1700 rpm for 5 min, poured onto clean, dust-free soda-lime glass plates, and spread with a doctor blade (16-mil blade gap) to obtain films having an average final thickness of 35.5 μm. The films were B-staged at 80 °C for 20 min with subsequent drying and thermal imidization in a forced-air oven at 100, 200, and 300 °C each for 1 h. After cooling to room temperature the polyimide films were removed from the glass plate by soaking in distilled water. The cobalt/lithium-codoped films were removed from the glass plate without immersion in water. In the following discussion the surface of the film in contact with the glass plate during imidization is referred to as the glass side while the surface in contact with the atmosphere of the forced-air oven is referred to as the air side of the film.

Spectroscopic Methods. X-ray photoelectron spectra were recorded with a Perkin-Elmer Phi Model 530 ESCA system. Auger electron spectra were recorded with a Perkin-Elmer Phi Model 610 scanning Auger microprobe system. X-ray photoelectron and Auger electron depth profile spectra were obtained via argon ion etching.

Thermal Methods. Thermogravimetric analyses were performed with a Perkin-Elmer Model TGS-2 thermogravimetric system at 10 °C/min heating rate with (50 cm/min) dynamic air purge.

Electrical Methods. Room-temperature surface and volume direct current electrical resistivities of 85-mm-diameter polymer films were determined with a Keithley high-voltage source (Model 240A), a Keithley electrometer (Model 610C), and a Keithley three-probe electrode assembly (Model 6105 resistivity adapter). Room-temperature charge vs. time (Q–t) measurements were obtained by using the Keithley 610C in the coulombmeter mode. Variable-temperature electrical resistivity determinations (VTERM) were obtained with a computer-controlled instrument developed in our laboratory.[10] The system controls sample temperature, atmosphere, electrification time, and measurement mode. The electrode geometry for the variable-temperature test cell is the same as the Keithley resistivity adapter.

Results and Discussion

Polyimide films modified with metal ions[11,12] and cured to a final temperature of 300 °C in air are generally colored but transparent, flexible, and strong and usually retain

0024-9297/87/2220-0790$01.50/0

Table I
Physical Properties of Cobalt- and Lithium-Modified Polyimide Films

polym system[a] BTDA/ODA/ $CoCl_2$/LiCl	film thickness,[b] μm	flexibility[c]	air-side charging characteristics	PDT,[d] °C
4/4/0/0	35.6	flexible	dielectric	553
4/4/1/0	38.9	flexible	conductor	476
4/4/1/0.005	33.5	flexible	conductor	477
4/4/1/0.05	36.1	flexible	dielectric	476, 473
4/4/1/0.5	33.5	flexible	conductor	464
4/4/0/1	31.0	brittle	conductor	488

[a] Number of moles of each component charged to the reactor. [b] Average of five measurements. [c] Qualitative fingernail crease test. [d] 10% mass loss, polymer decomposition temperature.

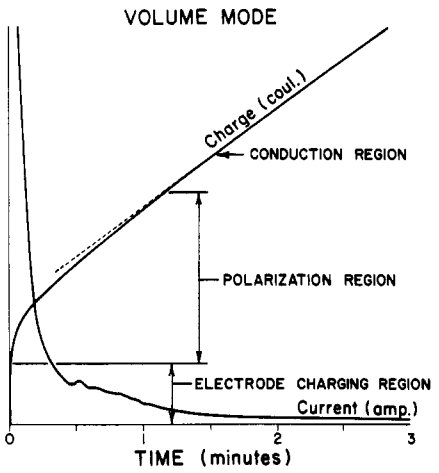

Figure 1. Typical volume mode charge–time and current–time profile for a metal ion modified polyimide film cured in air.

fairly high thermal stability. Data pertaining to the condensation polyimide films discussed in this report are shown in Table I. It appears that lithium or cobalt ion incorporation does decrease the thermal stability of the polyimide slightly compared with the nondoped control. For comparable additive levels cobalt decreases the thermal stability more than lithium, and the codoped film having the highest lithium content has the lowest stability. It is not clear if cobalt and lithium are acting synergistically to reduce the polyimide thermal stability or if the lower thermal stability of the codoped polyimides is due to the higher overall ionic content in the codoped vs. singly doped films.

Room-temperature direct current electrical resistivity values were determined via the three-probe guarded technique by measuring the current resulting from application of a +100 VDC step. The measured current, applied voltage, cell geometry, and measured sample thickness permit calculation of the volume (bulk) or surface (air side or glass side) electrical resistivity. For the Keithley 6105 resistivity adapter the pertinent equations are[13]

$$\rho_v = 22.9V/(dI)\ \Omega\ \text{cm}$$

$$\rho_s = 53.4V/I\ \Omega$$

where ρ_v is the volume resistivity in ohm centimeters, ρ_s is the surface (sheet) resistivity in ohms, V is the applied voltage in volts, I is the measured current in amperes, d is the sample film thickness in centimeters, and 22.9 cm^2 and 53.4 are the volume mode and the surface mode cell constants, respectively. A delay of at least 5 min prior to obtaining the current reading for both the glass side and

Table II
Resistivity of Lithium/Cobalt-Codoped Condensation Polyimide Films at Room Temperature

polym system[a] BTDA/ODA/ $CoCl_2$/LiCl	log (resistivity)[b] vol, Ω cm air	vol, Ω cm vacuum	air side, Ω air	air side, Ω vacuum	glass side, Ω air
4/4/0/0	17.60	17.60	16.28	17.76	16.00
4/4/1/0	17.61	16.57	12.55	12.55	16.07
4/4/1/0.005	14.57	~17.4	12.00	12.91	12.54
4/4/1/0.05	14.98	~17.3	11.87	15.01	15.99
4/4/1/0.5	11.72	16.30	12.29	12.12	11.86
4/4/0/1	14.41	17.16	14.06	>16.00	14.33

[a] Number of moles of each component charged to the reactor. [b] +100 VDC applied, measurement time ≥ 5 min, T = 25–27 °C.

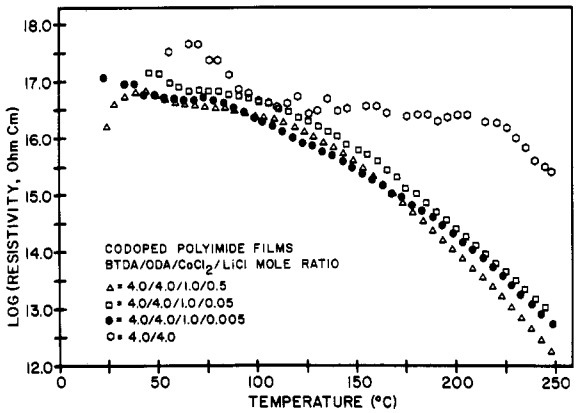

Figure 2. Volume mode dc electrical resistivity vs. temperature of lithium/cobalt-codoped BTDA/ODA polyimide films.

volume modes was considered necessary in these measurements because the charge–time profiles for these materials indicate instantaneous polarization, time-dependent polarization, and substantial dc conduction current (Figure 1). It is the third region upon which the data in this paper are based. This is in agreement with previous work of Sacher[14] in which steady-state, rather than transient, currents[15] were used to obtain information about the nature of charge transport in polyimides.

The room-temperature electrical resistivity data obtained in air for each measurement mode indicate that incorporation of metal salts results in reduced electrical resistivity for each lithium-doped and codoped film (Table II). In the case of the cobalt-doped film, only a reduced air-side resistivity is observed compared with the BTDA/ODA control. The measurements (in air) also indicate that the air-side resistivity is reduced more for the codoped films than for either of the singly metal ion doped films. Additional details are obtained by analysis at room temperature under vacuum. It is obvious from the data that the reduced *volume* mode electrical resistivity measured in air is not an intrinsic characteristic of the polymer but instead a result of the sample measurement atmosphere. Absorbed volatile species, predominantly moisture,[16–19] are thought responsible for the initially lower volume electrical resistivity. In support of this assignment, it has been demonstrated by microbalance techniques[20] and Fourier transform infrared spectroscopy[5] that lithium-doped BTDA/ODA films absorb water from the laboratory atmosphere. Similar results are also observed for the *air side* of the lithium-doped and codoped (0.05–mol lithium level) films.

Direct current electrical resistivity for the air side and volume modes evaluated under vacuum at elevated temperature allows more accurate sample comparisons.[21] The first heating cycle under vacuum (Figure 2) indicates that

Table III
Activation Energies for Conduction in Cobalt- and Lithium-Modified Polyimides

polym system[a] BTDA/ODA/ $CoCL_2$/LiCl	activation energy, kcal/mol	
	vol mode,[b]	air side
4/4/1/0	47.0	15.1
4/4/1/0.005	34.2 (0.994)	15.8 (0.996)
4/4/1/0.05	30.7 (0.996)	17.1 (0.997)
4/4/1/0.5	32.7 (0.997)	13.7 (0.999)

[a] Number of moles of each component charged to the reactor. [b] Data taken from the linear region below 250 °C (log ρ_v vs. $1/T$), first heating cycle. Numbers in parentheses are R^2, coefficient of correlation.

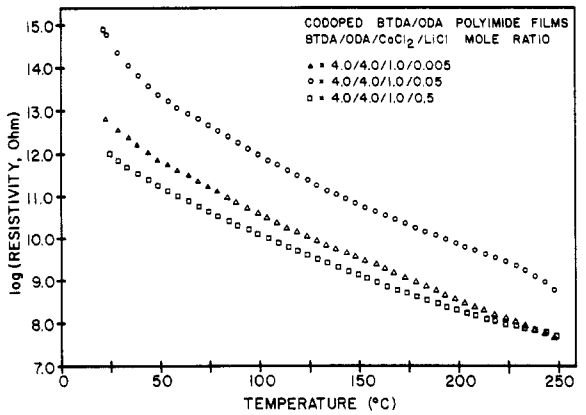

Figure 3. Air-side dc electrical resistivity vs. temperature of lithium/cobalt-codoped BTDA/ODA polyimide films.

each of the codoped samples has similar volume mode dc electrical resistivity (to within $^1/_2$ order of magnitude). The resistivity (Figure 2) is, however, more than 3 orders of magnitude lower (at 250 °C) than that observed for a nondoped BTDA/ODA polyimide film. Due to the method of film preparation it is likely that the decreased bulk resistivity is due to a larger number of charge carriers (a portion of dissociated metal salt) in the doped samples compared with the nondoped control. Very little hysteresis is noted when, for a particular sample, first heating–cooling and second heating–cooling profiles are compared. This implies that over the time range of the experiment (14.5 h) the sample has not been depleted of bulk charge carriers. The qualitative nature of the volume resistivity–temperature profiles (decreasing resistivity with increasing temperature) for the modified polyimides categorizes them as semiconductors or insulators. The influence of moisture on the volume mode electrical properties implies ionic conduction predominates. The activation energy for conduction, estimated from the slope of log (resistivity) vs. reciprocal temperature plots, supports ionic conduction in that the activation energy values obtained are always greater than 25 kcal/mol, Table III. Taylor,[19] on the basis of the energy of charge separation for ionic species in low dielectric constant materials, shows that, in general, ionic conduction should have an activation energy greater than 25 kcal/mol.

The qualitative nature of the air-side resistivity–temperature profiles (Figure 3) for the ion-modified polyimides also categorizes them as semiconductors or insulators, whereas the magnitude of the resistivity initially only categorizes them as insulators. These results seem to be inconsistent since in general no instantaneous polarization and no time-dependent polarization current was observed (Figure 4). The air side of the codoped film containing 0.05 mol of lithium chloride was the only sample that showed initial polarization current (Figure 4E). Polarization current is expected for this sample because the air-side variable-temperature electrical resistivity profile has curvature (due to a polymer influence) and the resistivity for the sample is 2–3 orders of magnitude higher than that for the other two codoped specimens. The lack of dielectric response in the air-side charge-time profiles for the majority of these films suggests that the air side is actually a semiconductor. The lower air-side electrical resistivity (compared with volume or glass side) for cobalt-doped polyimides was previously explained[6] in part by X-ray photoelectron spectroscopic results, which indicate the presence of a substantial amount of Co_3O_4 on the air side but a very low concentration of cobalt on the glass side for a variety of cobalt-modified films. Auger electron argon ion depth profiles support the notion that a high concentration of both cobalt and oxygen exists near the air side of the film while on the glass side only a small but constant concentration of cobalt and oxygen is revealed. The equation $\rho_v = \rho_s d$ can be used to estimate the bulk resistivity of the air-side oxide layer provided surface resistivity and oxide layer thickness are known. Such a calculation is valid because the Auger depth profile and electrical resistivity measurements (air side compared with volume) indicate that air-cured metal ion modified polyimide films are highly anisotropic. For example the measured surface resistivity of a cobalt chloride modified polyimide film is 1.12×10^{12} Ω at room temperature, which results in a calculated bulk resistivity of 1.51×10^7 Ω cm based on a cobalt oxide thickness of 1350 Å. The bulk resistivity of the surface oxide is therefore found to be numerically comparable to values for typical semiconductors. Koumoto and Yanagida[8] have measured the bulk electrical resistivity of Co_3O_4 (99.99% purity) in the temperature range 200–900 °C. Extrapolation of their data in the region between 200 and 320 °C (Figure 1 of ref 8) to 25 °C results in a value of 1.2×10^8 Ω cm, which compares favorably with our calculated value for several films. Other workers report values of 10^3–10^4 Ω cm[7,22,23] for the bulk resistivity of Co_3O_4. Preparation technique, purity, method of analysis, and oxide structure may each influence the apparent bulk resistivity. Activation energy plots (Figure 5) for the air-side surface resistivity of cobalt/lithium-modified BTDA–ODA polyimides indicate the activation energy for conduction is lower than 25 kcal/mol,

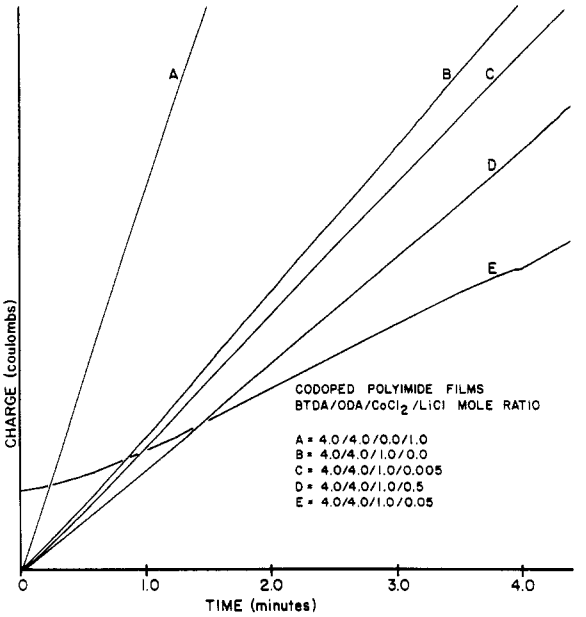

Figure 4. Air-side charge–time profiles for cobalt/lithium-codoped BTDA/ODA polyimide films.

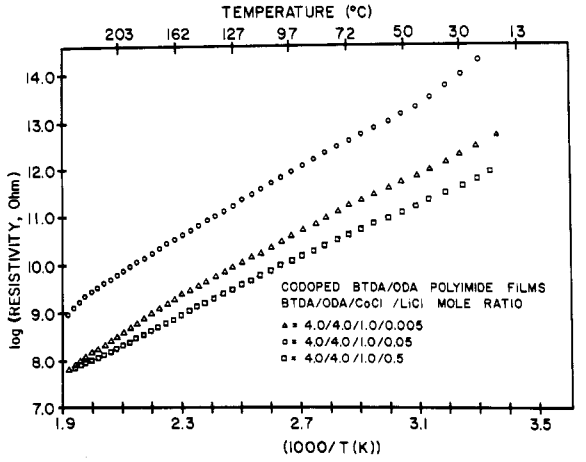

Figure 5. Activation energy plots for air-side electrical resistivity in cobalt/lithium-codoped BTDA/ODA polyimide films.

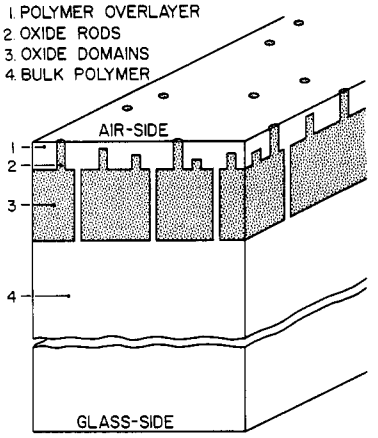

Figure 6. Structural model for cobalt-modified condensation polyimide films.

supportive of electronic semiconduction, Table III. The average value for a series of cobalt-doped condensation polyimides was found to be 13.5 kcal/mol, in good agreement with the work of Koumoto and Yanagida[8] (0.451 eV, 10.40 kcal/mol).

On the basis of the electrical and spectroscopic data, a structural model (Figure 6) for the cobalt chloride modified polyimides can be envisioned. We view the films as being composed of three units: (1) the bulk polymer film, containing cobalt(II) ion (i.e., dopant state) in a predominantly polyimide environment, (2) an "air-side" layer of Co_3O_4 with trace polyimide, and (3) a surface region, termed the "overlayer", containing a gradient of Co_3O_4 but primarily polyimide. The slightly lower bulk resistivity and higher dielectric constant for the doped films support our assignment for layer 1. That the air-side resistivity increases above the polyimide T_g as occurs in metal-filled polymer systems lends credence to layer 2. Controlled ion milling coupled with atomic concentration analysis of the milled area via XPS and AES confirm the polyimide–Co_3O_4 gradient overlayer. Air-side XPS photopeaks for carbon, imide oxygen, and nitrogen obtained prior to ion milling confirm the presence of polyimide at the surface. Data that support the presence of a polymer overlayer are found in Table IV. . The data indicate that signals due to polyimide (C and N) decrease with increasing sampling depth while that due to the additive (Co) increases. Overall, the oxygen photopeak signal having a contribution from both the polyimide oxygens and the cobalt oxide increases with increasing sampling depth. However, as shown in Figure 7 the deconvoluted oxygen peak indicates that organic

Table IV
XPS Depth Profile Data for a Cobalt-Modified BTDA/ODA Polyimide

	atomic concn, %			
est depth, Å	C	Co	N	O
100	57.8	13.4	3.1	25.7
200	52.6	17.7	2.6	27.1
300	48.9	22.5	2.2	26.5
400	46.5	24.5	2.3	26.9

Table V
XPS Data for Cobalt Photopeak in Cobalt/Lithium-Codoped Polyimide

polym system,[a] BTDA/ODA/ $CoCl_2$/LiCl	peak separation ($2p_{3/2}$ – $2p_{1/2}$), eV	Co $2p_{3/2}$, eV binding energy[b]
4/4/1/0.005	15.4	780.3
4/4/1/0.05	15.9	780.6
4/4/1/0.5	15.2	780.3

[a] Number of moles of each component charged to the reactor. [b] Corrected to aromatic carbon peak binding energy: C_{1s} = 284.6 eV.

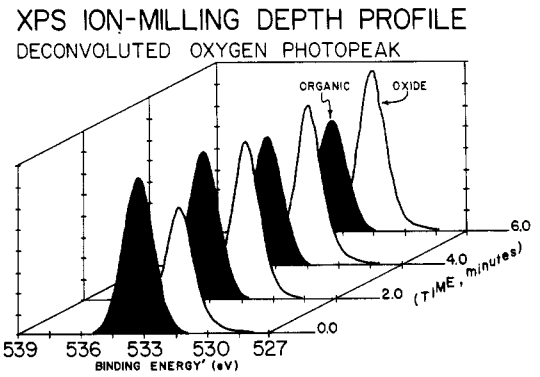

Figure 7. Deconvoluted oxygen photopeak from XPS–depth profile of a cobalt-modified polyimide film.

oxygen (higher binding energy) decreases but oxide oxygen (lower binding energy) increases with increasing sampling depth.

This model has been useful in that we realize lower surface resistivity may be attained by making the Co_3O_4 layer thicker. However, thicker oxide films will be more brittle and possibly too opaque. Ceramic technology suggests lithium substitution within the normal spinel structure of Co_3O_4 results in bulk resistivities up to a million times lower than that of pure Co_3O_4. The cobalt/lithium-codoped films that we have prepared may have incorporated this feature. The results are supportive of the proposed structural model developed for cobalt-modified condensation polyimides both in terms of spectroscopic (AES and XPS) and electrical properties (Q–t, and VTERM). Again, anisotropy is evident in these codoped films based on Auger electron argon ion depth profile data and charge–time profiles. Both lithium and cobalt are detected in a polymer overlayer that resides above a layer of predominantly "metal oxide". The bulk resistivity of the air side is reduced for two of the doped oxide films compared with pure Co_3O_4, Table II. The electrical properties can be explained on the basis of the XPS analysis of the cobalt $2p_{1/2}$ and $2p_{3/2}$ photopeaks. The data (Table V) indicate that the peak separation for the sample doped with 0.05 mol of lithium chloride has the largest peak separation between the two main photopeaks and shows intense satellite structure, Figure 8b. It is known that high-spin cobalt(II) compounds display in-

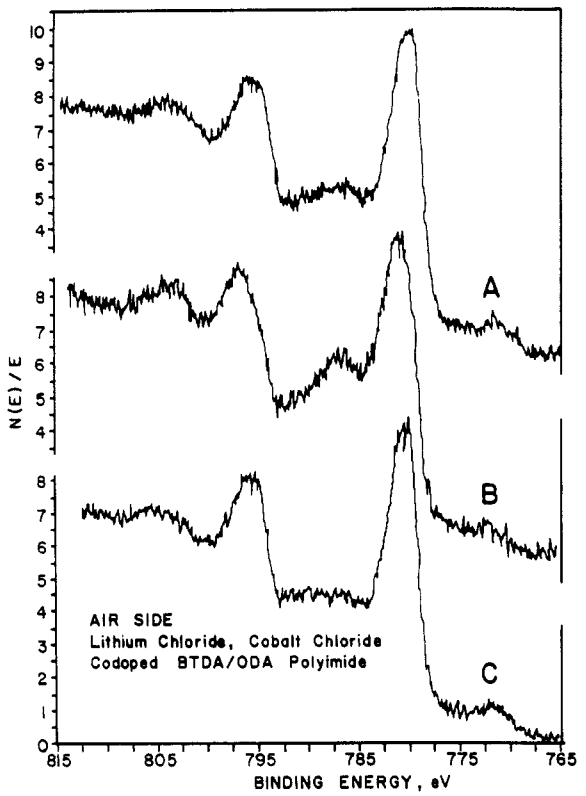

Figure 8. Cobalt photopeak from XPS analysis of cobalt/lithium-codoped polyimide film: (a) 0.005, (b) 0.05, and (c) 0.5 mol of lithium chloride.

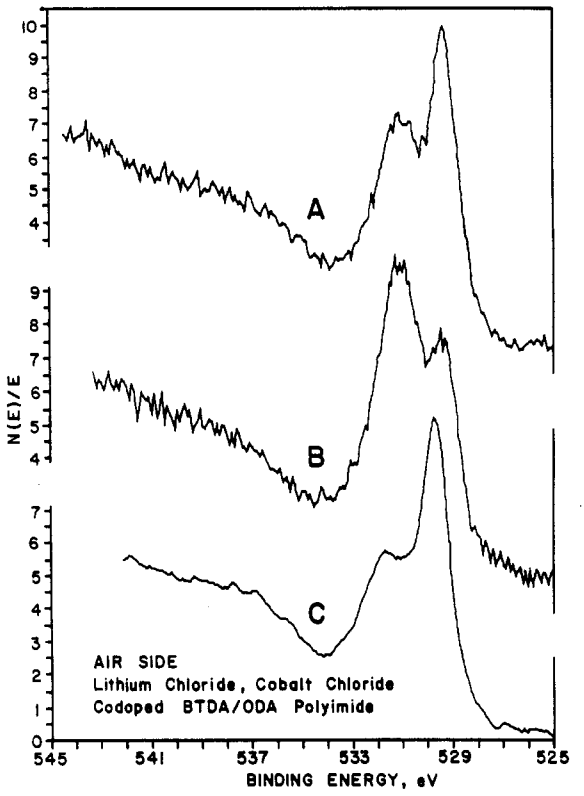

Figure 9. Oxygen photopeak from XPS analysis of cobalt/lithium-codoped polyimide films: (a) 0.005, (b) 0.05, and (C) 0.5 mol of lithium chloride.

tense satellite peak structure on the high binding energy side of the main photopeaks and that main peak separation is close to 16 eV. On the other hand, low-spin cobalt(III) compounds have main peak separation closer to 15 eV and show no satellite structure. XPS analysis of the film doped with 0.005 mol of lithium chloride (Figure 8a) indicates some satellite structure and main peak separation of 15.4 eV. Co_3O_4, $Co^{III}_2Co^{II}O_4$, gives a contribution from cobalt(III) but also from cobalt(II). Thus, an XPS spectrum indicative of each chemical species is expected. The third sample (doped with 0.5 mol of lithium chloride) shows a substantially different XPS spectrum, Figure 8c. Now, satellite structure is nearly absent and peak separation is closer to 15 eV as would be expected upon substantial substitution of Li^+ into the tetrahedral positions previously occupied by cobalt(II), thereby creating a spinel of general formula

$$(Li^{1+}_x Co^{2+}_{1-2x} Co^{3+}_x)_t (Co^{3+}_2)_o O_4$$

where subscripts t and o denote tetrahedral and octahedral lattice occupancy, respectively. Furthermore in order to maintain charge balance for each Co(II) substituted with lithium, another Co(II) must be oxidized to Co(III). Photoreduction of the sample in the spectrometer is always a potential source of artifacts. Photoreduction of the surface containing Co(III) would result in cobalt(II) and the emergence of satellite structure. For our cobalt-modified samples photoreduction does not seem to be significant. If it were, satellite structure should be more intense in Figure 8a than in Figure 8b (opposite of actual spectra) because the signal accumulation times were 29 and 21 min, respectively.

Evaluation of the oxygen XPS photopeak region (Figure 9) for each codoped sample shows that the samples containing the most and least amount of lithium exhibit a large amount of oxide oxygen observed at lower binding energy relative to the organic oxygen from the polymer matrix, in contrast to the intermediate lithium level film in which a smaller oxide oxygen peak is observed.

Table VI
XPS Depth Profile Data for a Cobalt/Lithium (1.0/0.5)-Codoped BTDA/ODA Polyimide Film

	atomic concn %				
est depth, Å	C	N	O	Co	Li
0	61.79	0.58	16.88	6.48	14.28
20	49.59	2.12	16.26	11.37	20.66
40	48.23	2.23	16.77	13.16	19.61
60	45.96	1.70	16.98	14.09	21.27
80	45.43	1.30	16.63	13.05	23.59

XPS depth profile data for a codoped film (containing 0.5 mol of lithium) supports the postulation of an overlayer similar to the singly doped cobalt films. Again, signals arising from the polymer decrease with increasing sampling depth while signals indicative of metal ion or oxide increase with increasing sampling depth, Table VI.

On the basis of the spectroscopic and electrical data, it appears that the film codoped with 0.005 mol of lithium chloride contains primarily Co_3O_4 on the air side and the one codoped with 0.05 mol of lithium chloride contains metal oxide and a substantial amount of residual ionic cobalt(II). Auger electron spectroscopy only shows a peak at 182 eV, corresponding to chlorine, in this intermediate level lithium codoped film, as expected. The film codoped with 0.5 mol of lithium chloride contains predominantly lithium-substituted cobalt oxide. Auger electron argon ion depth profile experiments showed that this codoped film contains a high level of lithium near the air side of the film in the same region in which cobalt and oxygen concentrations are also both high.

Additional cobalt additives and other polyimides of varying T_gs are being prepared and characterized. Other pure metal oxide spinels and substituted (Li, Zn, Ni, Fe,

Mn, Cu, etc.) oxide spinel structures in condensation and soluble polyimides are being pursued. Process parameters are also being probed to optimize the air-side oxide thickness, uniformity, and purity and to establish general structure–property–process correlations for metal ion modified polyimides. The model is being further probed by optical and electron microscopy and will be evaluated using ac electrical measurements.

Acknowledgment. We gratefully acknowledge the National Aeronautics and Space Administration for sponsoring this research, Leslie Horning for preparation of codoped films, Frank Cromer for his expertise and patience in performing the surface analysis, and Dr. Larry C. Burton (VPI & SU, Department of Electrical Engineering) for helpful suggestions and comments.

Registry No. BDTA-ODA polymer entry, 24980-39-0; BDTA-ODA SRU entry, 24991-11-5; Co, 7440-48-4; Li, 7439-93-2.

References and Notes

(1) Furtsch, T. A.; Taylor, L. T.; Fritz, T. W.; Fortner, G.; Khor, E. *J. Polym. Sci., Polym. Chem. Ed.* **1982**, *20*, 1287.
(2) Ezzell, S. A.; Taylor, L. T. *Macromolecules* **1984**, *17*, 1627.
(3) Boggess, R. K.; Taylor, L. T. *J. Polym. Sci., Polym. Chem. Ed.*, in press.
(4) Rancourt, J. D.; Boggess, R. K.; Taylor, L. T. *Polym. Mater. Sci. Eng.* **1985**, *53*, 74.
(5) Khor, E.; Taylor, L. T. *Macromolecules* **1982**, *15*, 379.
(6) Rancourt, J. D.; Boggess, R. K.; Horning, L. S.; Taylor, L. T. *J. Electrochem. Soc.*, in press.
(7) Appandairajan, N. K.; Viswanathan, B.; Gopalakrishnan, J. *J. Solid State Chem.* **1981**, *40*, 117.
(8) Koumoto, K.; Yanagida, H. *J. Am. Ceram. Soc.* **1981**, November, C-156.
(9) Rancourt, J. D.; Taylor, L. T. *Polym. Mater. Sci. Eng.* **1986**, *54*, 124.
(10) Rancourt, J. D.; Swartzentruber, J. L.; Taylor, L. T. *Am. Lab. (Fairfield, Conn.)* **1986**, March.
(11) St. Clair, A. K.; Taylor, L. T. *J. Appl. Polym. Sci.* **1983**, *28*, 2393.
(12) Taylor, L. T.; St. Clair, A. K. *Polyimides*; Mittal, K. L., Ed.; Plenum: New York, 1984; Vol. 2; p 617.
(13) *Instruction Manual*, Model 6105 Resistivity Adapter; Keithley Instruments: Cleveland, OH.
(14) Sacher, E. *IEEE Trans. Electr. Insul.* **1979**, *EI-14* (2), 85.
(15) Hanscomb, J. R.; Calderwood, J. H. *J. Phys. D.* **1973**, *6*, 1093.
(16) Sacher, E.; Susko, J. R. *J. Appl. Polym. Sci.* **1979**, *23*, 2355.
(17) Barker, R. E., Jr. *Pure Appl. Chem.* **1976**, *46*, 157.
(18) Barker, R. E., Jr.; Sharbaugh, A. H. *J. Polym. Sci., Part C*, **1965**, *10*, 139.
(19) Taylor, C. P. S. *Nature (London)* **1961**, *189*, 388.
(20) Rancourt, J. D.; Taylor, L. T. *J. Therm. Anal.*, in press.
(21) Warfield, R. W. *Treatise on Analytical Chemistry*; Kolthoff, I. M. et al., Eds.; Wiley: New York, 1977; Vol. 4, Part III, p 615.
(22) Appandairajan, N. K.; Gopalakrishnan, J. *Proc. Indian Acad. Sci., Sect. A* **1978**, *87A*, 115.
(23) Rao, C. N. R.; Rao, G. V. S. *Transition Metal Oxides*; National Bureau of Standards; Gaithersburg, MD, 1972; NSRDS-NBS 49.

Study of Mobile and Rigid Peroxy Radicals in Polypropylene

M. G. Alonso-Amigo and Shulamith Schlick*

Department of Chemistry, University of Detroit, Detroit, Michigan 48221.
Received October 28, 1986

ABSTRACT: Two types of peroxy radicals have been obtained in polypropylene by γ irradiation and exposure to oxygen. The radicals differ in their dynamics and stability. The stable and rigid peroxy radical can be studied separately after the decay of the mobile radical. Reversible changes in the ESR spectra from the peroxy radicals have been studied from 77 to 303 K and assigned to g-tensor averaging due to motion. The principal values of the g tensor for both radicals at 77 K are 2.0349, 2.0069, and 2.0032. ESR spectra from both radicals are simulated by using the modified Bloch equations. Best agreement with experimental results is obtained by assigning to the mobile radical a chain axis rotation with 180° jumps and to the rigid radical a C–O bond rotation with 180° jumps. The simulations indicate that the angles between g_1, g_2, and g_3 in the mobile radical and the chain axis are 50°, 97°, and 41°, respectively. g_1 is in the direction of the O–O bond, and g_3 is perpendicular to the COO plane. Inspection of the spectra from polypropylene γ irradiated under vacuum suggests that the most likely precursors for the rigid and mobile peroxy radicals are the midchain radical $-CH_2\dot{C}(CH_3)CH_2-$ and the end-chain or propagating, radical $-CH_2CH(CH_3)CH_2^{\bullet}$, respectively. An additional end-chain radical, $-CH_2\dot{C}H(CH_3)$, is also formed on γ irradiation. No significant effect of the degree of crystallinity on the ESR spectra or intensity ratio of the two radicals has been detected.

Introduction

The radiation chemistry of polypropylene (PP) has been extensively investigated in recent years.[1-9] Samples irradiated under vacuum have indicated the presence of several alkyl radicals which have been studied by ESR spectroscopy in polypropylenes with different degrees of crystallinity. It has been suggested that most of these alkyl radicals are located in the crystalline portions of the samples, thus explaining the considerable stability of the radicals in the absence of oxygen.[5,7]

High-energy irradiation of PP in air, or exposure of the alkyl radicals formed under vacuum to oxygen, results in formation of peroxy radicals. These radicals were also studied by ESR and identified by their typical g anisotropy and lack of hyperfine interaction. In contrast to alkyl radicals, however, the peroxy radicals in PP decay at room temperature within several days and even faster when the temperature is increased to 310 K. It has been suggested that peroxy radicals are localized in the amorphous regions of the polymer.[5,10] The kinetics of the peroxy radical decay in PP has been widely studied, because polymer oxidation results in degradation and in change in the mechanical properties on which the use of PP is based.[2]

ESR studies have also indicated that *two* types of peroxy radicals are formed in PP, with different mobilities and stabilities. The "rigid" peroxy radicals have been studied by Suryanarayana and Kevan[8] in terms of a specific motional mechanism. Both types of radicals have been studied by Kashiwabara and co-workers.[9] The main conclusions from these studies were that the mobile peroxy

0024-9297/87/2220-0795$01.50/0